[CANCER RESEARCH 62, 7213–7218, December 15, 2002]

Advances in Brief

Dependence of Histone Modifications and Gene Expression on DNA Hypermethylation in Cancer[1,2]

Jill A. Fahrner,[3] Sayaka Eguchi,[3] James G. Herman, and Stephen B. Baylin[4]

The Sidney Kimmel Comprehensive Cancer Center at Johns Hopkins University, Baltimore, Maryland 21231-1000 [J. A. F., S. E., J. G. H., S. B. B.], and The Graduate Program in Cellular and Molecular Medicine, The Johns Hopkins University School of Medicine, Baltimore, Maryland 21231 [J. A. F., S. E., J. G. H., S. B. B.]

Abstract

We examined the relationship between aberrant DNA hypermethylation and key histone code components at a hypermethylated, silenced tumor suppressor gene promoter in human cancer. In lower eukaryotes, methylated H3-lysine 9 (methyl-H3-K9) determines DNA methylation and correlates with repressed gene transcription. Here we show that a zone of deacetylated histone H3 plus methyl-H3-K9 surrounds a hypermethylated, silenced *hMLH1* promoter, which, when unmethylated and active, is embedded in methyl-H3-K4 and acetylated H3. Inhibiting DNA methyltransferases, but not histone deacetylases, leads first to promoter demethylation, second to gene reexpression, and finally to complete histone code reversal. Our findings suggest a new paradigm-DNA methylation may directly, or indirectly by inhibiting transcription, maintain key repressive elements of the histone code at a hypermethylated gene promoter in cancer.

Introduction

Aberrant promoter DNA hypermethylation and associated epigenetic gene silencing frequently provide for loss of tumor suppressor gene function in cancer (1, 2). DNA methylation-mediated gene silencing is closely linked to the deacetylation of histones (1, 2). More recently, methylation of histones at key lysine residues has been shown to work in concert with acetylation and other modifications to provide a histone code that may determine heritable transcriptional states (3). The data for this have come predominantly from studies examining broad domains in chickens (4), yeast (5), and the mammalian inactive X chromosome (6–8), as well as individual promoter sites known to be expressed or silenced by epigenetic mechanisms such as X inactivation (8) and genomic imprinting (9). These studies reveal that acetylated histone H3 and methyl-H3-K4[5] are enriched in euchromatic domains and correlate with active gene expression, whereas methyl-H3-K9 is enriched at deacetylated, transcriptionally silent heterochromatic regions (4–9).

The above histone modifications have been widely hypothesized to determine active *versus* inactive gene expression status (4–9). Moreover, presence of methyl-H3-K9 has recently been shown to be essential for all or a subset of DNA methylation in *Neurospora crassa* (10) and *Arabidopsis thaliana* (11), respectively. However, for hypermethylated tumor suppressor genes in human cancer, DNA hypermethylation appears to be dominant over at least the histone deacetylation part of the histone code for maintaining a silenced state (12). In this regard, we have shown previously that the DNA demethylating agent 5-Aza-dC, but not the HDAC inhibitor TSA, reactivates the expression of such genes (12, 13). We now provide evidence that promoter DNA hypermethylation can control transcriptional silencing and, either directly or indirectly, the state of key elements of the histone code. At *hMLH1*, a mismatch repair gene often silenced with aberrant CpG island hypermethylation in colorectal cancers (14), a zone of deacetylated H3 (deacetylated histone H3-K9 and -K14) plus methyl-H3-K9 (dimethyl-H3-K9) surrounds the hypermethylated, silenced promoter. This same promoter, when unmethylated and active, is embedded in methyl-H3-K4 (dimethyl-H3-K4) and acetylated H3 (acetylated histone H3-K9 and -K14). Treatment with TSA fails to reactivate the hypermethylated gene or dramatically alters the histone modifications examined. However, 5-Aza-dC treatment leads to initiation of demethylation by 12 h, appearance of transcription by 24 h, and full reversal of key elements of the histone code by 48 h. Thus, DNA hypermethylation, either directly or indirectly through suppressing transcription, appears to specify for repressive histone modifications at a tumor suppressor gene promoter. An important element of the findings is that the demethylating drug 5-Aza-dC appears to be a potent tool for dissecting the components of this DNA methylation-mediated transcriptional control and for potentially reversing their interaction for therapeutic purposes in cancer.

Materials and Methods

Cell Culture. SW480 cells were maintained in McCoy's 5A modified medium. RKO cells were maintained in MEM. All media (Invitrogen) were supplemented with 10% fetal bovine serum (Gemini Bio-Products) and 1% penicillin/streptomycin (Invitrogen) and grown at 37°C in 5% CO_2 atmosphere.

5-Aza-dC and TSA Treatments. Cells were treated with mock or 1 μM 5-Aza-dC (Sigma) for 12, 24, 48 h, or 5 days or with 300 nM TSA (Wako) for 24 h, as described previously (12, 14).

ChIP. We used the ChIP Assay Kit from Upstate Biotechnology and followed the manufacturer's protocol with some modifications.

Briefly, proteins were cross-linked to DNA by addition of formaldehyde directly to the culture medium to a final concentration of 1% for 10 min at room temperature. The cross-linking reaction was quenched by adding glycine to a final concentration of 0.125 M for 5 min at room temperature. The medium was then removed and cells were washed with 1× PBS containing a combination of protease inhibitors (1 mM Pefabloc and 1× Complete protease inhibitor mixture; Roche Molecular Biochemicals). The PBS was removed and 0.2× trypsin was added to the cells. After a 5-min incubation at 37°C, ice-cold 1× PBS containing 10% FBS was added to stop trypsinization. The cells were scraped off the culture flask, pelleted, and washed twice with 1× PBS plus protease inhibitors as above. For each ChIP assay ~10^6 cells were used. The sonicated samples were precleared with 80 μl of salmon sperm DNA/Protein

Received 11/11/02; accepted 11/11/02.

The costs of publication of this article were defrayed in part by the payment of page charges. This article must therefore be hereby marked *advertisement* in accordance with 18 U.S.C. Section 1734 solely to indicate this fact.

[1] Supported by NIH Grant CA43318 from the National Cancer Institute and ES11858 from the National Institute of Environmental Health Sciences.

[2] J. G. H. and S. B. B. are consultants to Tibotec-Virco. Under licensing agreement between the Johns Hopkins University and Tibotec-Virco, MSP was licensed to Tibotec-Virco, and they are entitled to a share of the royalties received by the University from sales of the licensed technology. The terms of these arrangements are being managed by the University in accordance with its conflict of interest policies.

[3] These authors contributed equally to this work.

[4] To whom requests for reprints should be addressed, at The Sidney Kimmel Comprehensive Cancer Center at Johns Hopkins, Tumor Biology Laboratory, The Bunting-Blaustein Cancer Research Building, 1650 Orleans Street, Room 541, Baltimore, MD 21231-1000. Phone: (410) 955-8506; Fax: (410) 614-9884; E-mail: sbaylin@jhmi.edu.

[5] The abbreviations used are: methyl-H3-K4, methylated histone H3-lysine 4; methyl-H3-K9, methylated histone H3-lysine 9; DNMT, DNA methyltransferase; HDAC, histone deacetylase; 5-Aza-dC, 5-Aza-2′deoxycytidine; TSA, Trichostatin A; ChIP, chromatin immunoprecipitation; GAPDH, glyceraldehyde-3-phosphate dehydrogenase; MSP, methylation-specific PCR.

A and Protein G agarose beads (3:1 ratio of Protein A to Protein G; Upstate Biotechnology) for 1 h at 4°C with agitation. The soluble chromatin fraction was collected, and 5 μl of either anti-acetyl-Histone H3 (Lys 9 and Lys 14), anti-dimethyl-Histone H3 (Lys 4), anti-dimethyl-Histone H3 (Lys 9), or no antibody was added and incubated overnight with rotation (all antibodies from Upstate Biotechnology). Immune complexes were collected with 60 μl of the 3:1 salmon sperm DNA/Protein A and Protein G agarose beads. The beads were washed as recommended but were transferred to a new tube before each wash. After elution, the cross-links were reversed, and the samples were digested with proteinase K. DNA was recovered by phenol extraction, ethanol precipitated, and resuspended in 1× 10 mM Tris (pH 8)-1 mM EDTA buffer.

PCR Amplification and Analysis. Primer sets for PCR were designed to amplify overlapping fragments of ~200 bp along the *hMLH1* promoter. One primer set for *GAPDH* was designed to amplify a 128-bp fragment of the genomic sequence to serve as an internal control. All primers were purchased from Invitrogen or IDT. All PCR reactions were performed with JumpStart REDTaq DNA Polymerase (Sigma) in a total volume of 25 μl, using 1–2 μl of either immunoprecipitated (bound) DNA, a 1:10 dilution of nonimmunoprecipitated (input) DNA, or a no-antibody control. All reactions were optimized with input DNA to ensure that PCR products for both *hMLH1* and *GAPDH* were in the linear range of amplification. Primer sequences and additional PCR conditions are available upon request. Ten μl of PCR product were size fractionated by PAGE and were quantified using Kodak Digital Science 1D Image Analysis software. Enrichment was calculated by taking the ratio between the net intensity of the *hMLH1* PCR product from each primer set and the net intensity of the *GAPDH* PCR product for the bound sample and dividing this by the same ratio calculated for the input sample. Values for enrichment were calculated as the average from at least two independent ChIP experiments and multiple independent PCR analyses of each.

MSP. Genomic DNA was isolated using the Wizard Genomic DNA Purification Kit (Promega). The genomic DNA was modified by bisulfite treatment, as described previously (15). The primers used for MSP have been previously described (14) and were purchased from Invitrogen. Primer sequences and additional PCR conditions are available upon request.

Reverse Transcriptase-PCR. We isolated RNA with Trizol (Invitrogen), according to the manufacturer's instructions. RNA was reverse transcribed using Superscript II Rnase H Reverse Transcriptase (Invitrogen). PCR was performed using 1 μl of cDNA and primers unambiguous for *GAPDH* or *hMLH1* (Invitrogen). All PCR reactions were performed with JumpStart RED-Taq DNA Polymerase (Sigma) in a total volume of 25 μl. Primer sequences and additional PCR conditions are available upon request.

Results

Mapping the Histone Code at *hMLH1*. We compiled a detailed map of histone acetylation and histone methylation across a 1.8-kb region of the promoter for *hMLH1*. We performed ChIP for two human colorectal cancer cell lines, RKO and SW480, in which the *hMLH1* promoter is hypermethylated and transcriptionally silenced or unmethylated and transcriptionally active, respectively (14). The histone-associated DNA regions were analyzed using a multiplex PCR approach with overlapping primer sets spanning the promoter (Fig. 1*A*). Overall, acetylated histone H3 was enriched throughout the unmethylated *hMLH1* promoter; however, there was essentially no acetylation of these same sites along the hypermethylated promoter (Fig. 1, *B* and *C*). Virtually identical results were observed for methyl-H3-K4 at the two promoters (Fig. 1, *D* and *E*). In stark contrast, methyl-H3-K9 was enriched along the entire hypermethylated, silenced *hMLH1* promoter, especially over a region where it was depleted to virtually undetectable levels along the unmethylated, transcriptionally active promoter (Fig. 1, *F* and *G*). Thus, it seems that key elements of the histone code surrounding an aberrantly hypermethylated tumor suppressor gene in human cancer resemble the histone modifications that may be necessary for proper genomic imprinting and gene expression along the X chromosome in other

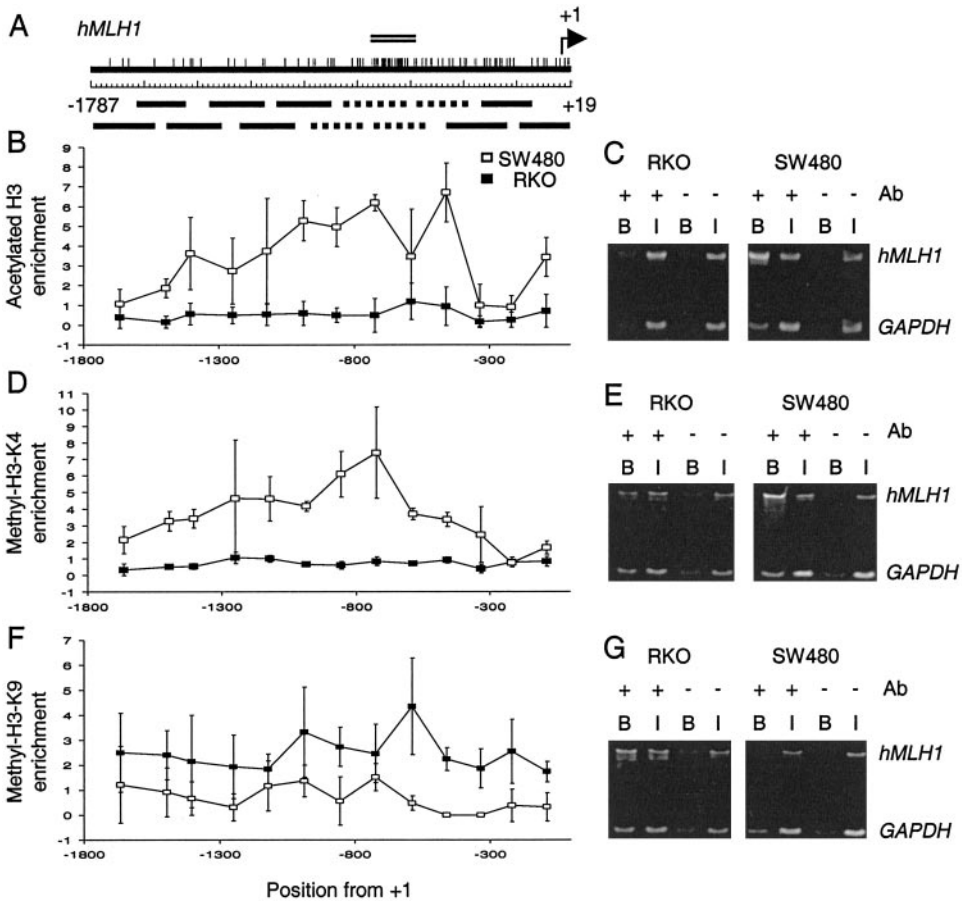

Fig. 1. Map of histone H3 modifications along a hypermethylated *versus* an unmethylated *hMLH1* promoter. *A*, schematic of the *hMLH1* promoter. The *vertical lines* represent the location of CpG dinucleotides, and the *arrow* indicates the approximate position of the transcription start site. The CpG island extends 3′ from ~−800 (relative to the transcription start site) into exon 1. The *doubled horizontal line* denotes the region examined by MSP. In SW480 cells, the promoter is unmethylated, and the gene is expressed. However in RKO cells, the promoter is hypermethylated, and the gene is silenced. The *horizontal bars* below the schematic indicate the location of the DNA fragments amplified by PCR done on the DNA recovered from ChIP experiments. The *broken bars* denote the primer sets used in the time course experiments. *B*, *D*, and *F*, enrichment of *hMLH1* promoter DNA immunoprecipitated with antibodies specific for acetylated histone H3 (K9 and K14), dimethyl-H3-K4, and dimethyl-H3-K9, respectively. *Points* on the graphs represent data from the corresponding DNA fragment amplified by PCR, as shown at the bottom *A*. The value of each point was calculated as the average from two independent ChIP experiments and a total of four independent PCR analyses. Each *error bar* indicates the SD from the mean. □ represent data from SW480. ■ represent data from RKO. *C*, *E*, and *G*, representative PCR analyses of ChIP on RKO and SW480 from areas typical of enrichment for acetylated H3, methyl-H3-K4, and methyl-H3-K9, respectively. Multiplex PCR was performed on bound (B) immunoprecipitated DNA and input (I) nonimmunoprecipitated DNA with each *hMLH1* primer set.

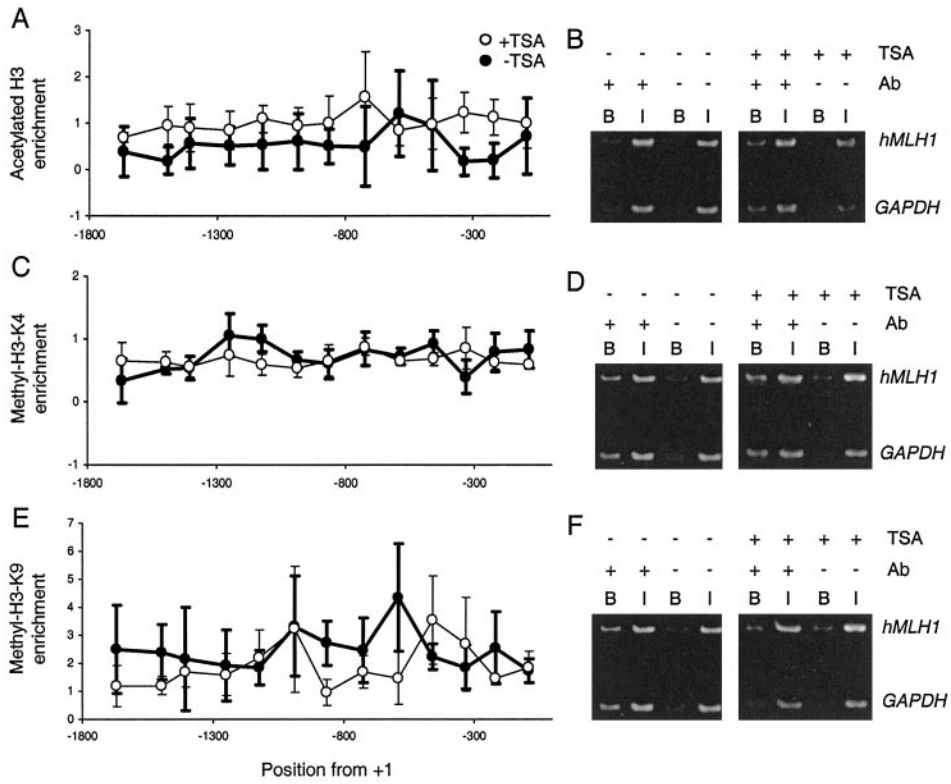

Fig. 2. Inhibition of histone deacetylation by TSA fails to dramatically alter key components of the histone code map along the hypermethylated *hMLH1* promoter. ChIP was done on RKO cells after treatment with 300 nM TSA for 24 h. *A*, *C*, and *E*, enrichment of acetylated histone H3 (K9 and K14), dimethyl-H3-K4, and dimethyl-H3-K9, respectively, at the *hMLH1* promoter. ○ represents enrichment in RKO cells treated with TSA. ● represents data from untreated RKO cells. *Points* on each graph represent data from the corresponding DNA fragment amplified by PCR, as illustrated in Fig. 1*A*. The value of each point was calculated as the average from two independent ChIP experiments and a total of four independent PCR analyses. Each *error bar* indicates the SD from the mean. *B*, *D*, and *F*, representative PCR analyses of ChIP performed on RKO cells, before and after treatment with TSA, from areas typical of enrichment for acetylated H3, methyl-H3-K4, and methyl-H3-K9, respectively. Bound DNA (B) and input DNA (I) were coamplified with primers for *hMLH1* and *GAPDH*.

mammalian cells (6–9) and for defining large heterochromatic and euchromatic domains in chickens (4) and yeast (5).

Inhibition of HDACs with TSA. Although little is known about the relationship between DNA methylation and the methylation component of the histone code in mammals, it has been known for some time that DNA methylation and histone deacetylation work in concert to silence genes in cancer (1, 2, 16, 17). In fact, we have shown previously that DNA methylation is dominant over histone deacetylation in maintaining a silent state at hypermethylated promoters because 5-Aza-dC can reactivate genes silenced with aberrant promoter hypermethylation but TSA alone cannot reactivate these same genes (12). We explored these findings further at the level of the histone code. We treated RKO cells with TSA, which alone did not reactivate *hMLH1*, but which was able to reactivate *FABP4*, a control gene silenced in these cells by a mechanism distinct from one involving DNA hypermethylation (Ref. 13; data not shown). Subsequent ChIP and PCR analysis revealed only a slight increase in acetylated H3 at the *hMLH1* promoter (Fig. 2, *A* and *B*) and essentially no change in methyl-H3-K4 (Fig. 2, *C* and *D*) and methyl-H3-K9 (Fig. 2, *E* and *F*). These data show that in addition to being unable to reactivate expression of a hypermethylated, silenced *hMLH1*gene, TSA alone is unable to evoke obvious changes in key parameters of the histone code at this promoter.

Inhibition of DNMTs with 5-Aza-dC. Recent genetic studies in *Arabidopsis* (11) and *Neurospora* (10) suggest that methyl-H3-K9 may determine sites of DNA methylation, although evidence for the existence of this relationship in higher eukaryotes has not been explored. We therefore set out to probe this relationship between key elements of the histone code and DNA methylation. We addressed this question by using ChIP and PCR analysis to examine the fate of histone modifications at the *hMLH1* promoter upon inhibition of DNMTs by a dose of 5-Aza-dC, which is sufficient to cause demethylation of the promoter region (14) and to reactivate the expression of the hypermethylated, silenced *hMLH1* gene in RKO cells (Ref. 14; data not shown). Surprisingly, after drug treatment, we observed a complete reversal of the histone code components examined at the *hMLH1* promoter in RKO cells. Acetylated H3 and methyl-H3-K4 levels became markedly enriched (Fig. 3, *A–D*), whereas methyl-H3-K9 levels were severely depleted (Fig. 3, *E* and *F*). Thus with 5-Aza-dC, we recapitulated in RKO cells the state of the unmethylated, expressed promoter originally observed in SW480 cells (compare Fig. 3, *A*, *C*, and *E* to Fig. 1, *B*, *D*, and *F*). This transformation of key parameters of the histone code upon inhibition of the DNMTs suggests that in human colorectal cancer cells, DNA hypermethylation, or another activity mediated by DNMTs, may be essential for maintaining a particular combination of histone modifications at gene promoters silenced with aberrant DNA hypermethylation. Furthermore, the observation that 5-Aza-dC, but not TSA, can both reactivate expression of the silenced *hMLH1* gene and completely reverse key histone modifications surrounding the gene promoter strengthens the idea that there exists some interdependence between reversal of important histone code components and reactivation of a gene silenced with aberrant DNA hypermethylation.

Time Course Analysis after 5-Aza-dC Treatment. The observation that inhibition of the DNMTs leads to both steady-state reactivation of *hMLH1* expression and complete reversal of key histone code parameters surrounding the gene promoter invited delineating the sequence of events to help dissect the operative mechanisms. We performed time course studies in which RKO cells were treated with 5-Aza-dC and monitored over 5 days for the states of key elements of the histone code, DNA methylation, and gene expression using ChIP and PCR analysis, MSP, and reverse transcriptase-PCR, respectively. For the ChIP and PCR analysis, we used four of the original 13 primer sets (Fig. 1*A*), which cover the region of greatest difference in histone modification observed between RKO and SW480 cells and also between 5-Aza-dC-treated and -untreated RKO cells at *hMLH1* (Fig. 1, *A*, *B*, *D*, and *F*; Fig. 3, *A*, *C*, and *E*). At 12 and 24 h after the start of 5-Aza-dC treatment, there was no dramatic change in the histone

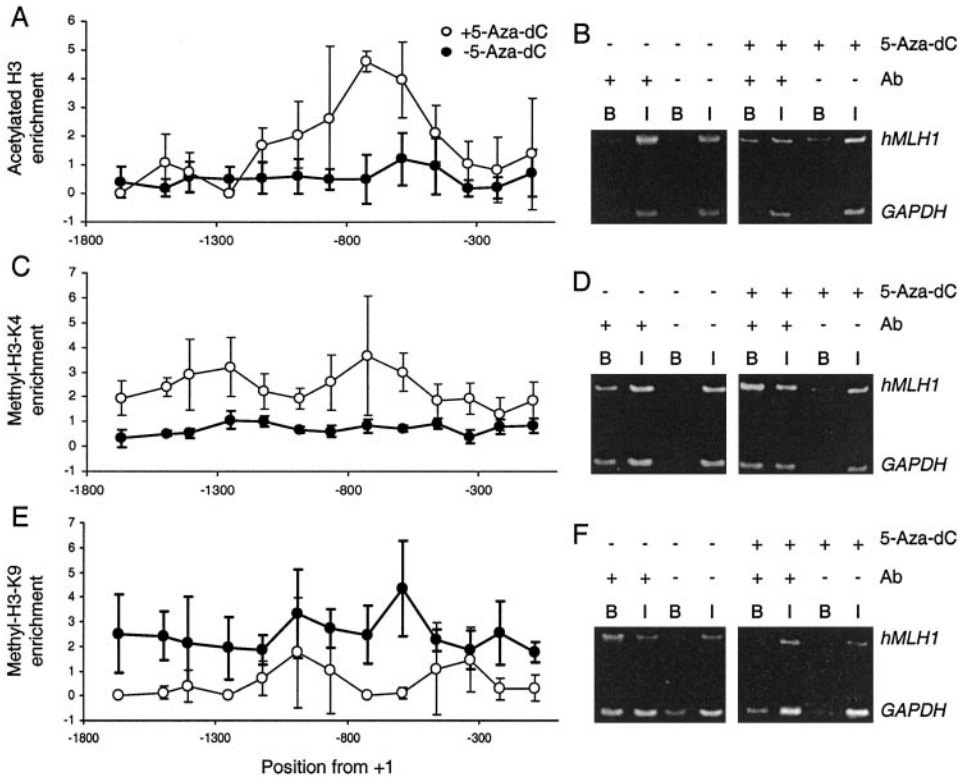

Fig. 3. Inhibition of DNA methylation by 5-Aza-dC completely reverses all examined components of the histone code map along the hypermethylated *hMLH1* promoter. ChIP was performed on RKO cells after treatment with 1 μM 5-Aza-dC for 5 days. *A*, *C*, and *E*, enrichment of *hMLH1* promoter DNA precipitated by antibodies specific for acetylated histone H3 (K9 and K14), dimethyl-H3-K4, and dimethyl-H3-K9, respectively. ○ represents enrichment in RKO cells treated with 5-Aza-dC. ● represents data from untreated RKO cells. The value of each point was calculated as the average from two (untreated) or three (drug-treated) independent ChIP experiments and four independent PCR analyses from each untreated or drug-treated experiment. Each *error bar* indicates the SD from the mean. *Points* on each graph correspond to the overlapping DNA fragments amplified by PCR as depicted in Fig. 1*A*. *B*, *D*, and *F*, representative PCR analyses of ChIP done on RKO cells, with or without treatment with 5-Aza-dC, from areas typical of enrichment for acetylated H3, methyl-H3-K4, and methyl-H3-K9, respectively. DNA from bound (B) and input (I) fractions were coamplified with primers for *hMLH1* and *GAPDH*.

code components examined (Fig. 4). By 48 h, acetylated H3 and methyl-H3-K4 showed dramatic enrichment in 5-Aza-dC-treated samples compared with mock-treated samples; at the same time, methyl-H3-K9 became depleted (Fig. 4). We next used MSP to examine the methylation status of the *hMLH1* promoter after treatment with 5-Aza-dC. The region examined covers the area of greatest CpG density in the promoter and overlaps with the region examined by ChIP and PCR analysis in these time course studies (Fig. 1*A*). By 12 h, we observed demethylation of the promoter, which was maximal by 24 h and sustained until 5 days after the start of drug treatment (Fig. 5*A*). Finally, we examined reexpression of *hMLH1* by 5-Aza-dC using reverse transcriptase-PCR. Transcriptional reactivation became apparent by 24 h after the start of 5-Aza-dC treatment, and gene expression continued throughout the time course (Fig. 5*B*). The observed sequence of events, then, is demethylation of the *hMLH1* promoter by 12 h, appearance of *hMLH1* transcript by 24 h, and complete reversal of all examined histone code components along the gene promoter by 48 h (Table 1).

Although in these experiments it appears that demethylation distinctly occurred first, as it was detectable by 12 h and maximal by 24 h, we are less certain about the order of events with respect to reactivation of transcription and reversal of the histone code parameters examined because of the different sensitivities of the techniques used. To help sort this out, we examined data from several immunofluorescence experiments in which we stained for hMLH1 protein after treatment of RKO cells for 24 h with the same dose of 5-Aza-dC used in the present studies. No nuclear staining was visible in mock-treated cells, but distinct reexpression of hMLH1 protein was present in 33–50% of RKO cells by 24 h (data not shown). These data suggest that a substantial percentage of cells were transcribing *hMLH1* by 24 h in our present time course experiments and that the ChIP procedures would likely have detected a distinct change in the histone code parameters examined if these changes had preceded transcription. Our data, then, suggest a sequence of events in which 5-Aza-dC produces demethylation first, transcriptional reactivation second, and reversal of important histone code components third.

Discussion

Our data provide the first detailed map of H3 acetylation and H3 methylation for a hypermethylated *versus* an unmethylated gene promoter in cancer cells. We also demonstrate here that inhibiting the DNMTs, but not the HDACs, essentially recapitulates at a hypermethylated, silenced promoter a combination of histone modifications similar to that at an unmethylated, active promoter. Finally, our results show unequivocally that DNA demethylation precedes both the reactivation of the silenced gene and, somewhat surprisingly, the reversal of key elements of the repressive histone code. These findings are consistent with the idea that DNA demethylation, either directly or indirectly by reactivating transcription of the *hMLH1* gene, reverses important components of the repressive histone code surrounding the hypermethylated promoter. These results favor the idea that DNA hypermethylation, not a particular combination of histone modifications containing elevated methyl-H3-K9, is the dominant epigenetic mechanism involved in maintaining silencing of the *hMLH1* gene.

In considering the mechanisms that underlie our observation that upon treatment with 5-Aza-dC, demethylation precedes reactivation of transcription, which precedes reversal of key histone code parameters, at least two scenarios may be considered. The first potential mechanism is one in which DNA methylation plays a direct role in both gene silencing and maintaining a repressive histone code at a hypermethylated gene promoter in cancer. We could speculate that the DNA modification itself, or components of the DNA methylating machinery such as the DNMTs or methyl-CpG binding proteins, could directly interact with histone methyltransferases or proteins that target them, directing them to regions containing DNA methylation and allowing them to set up a repressive histone code (18). If this turns out to be the case, it would suggest a new paradigm, seeing that data from

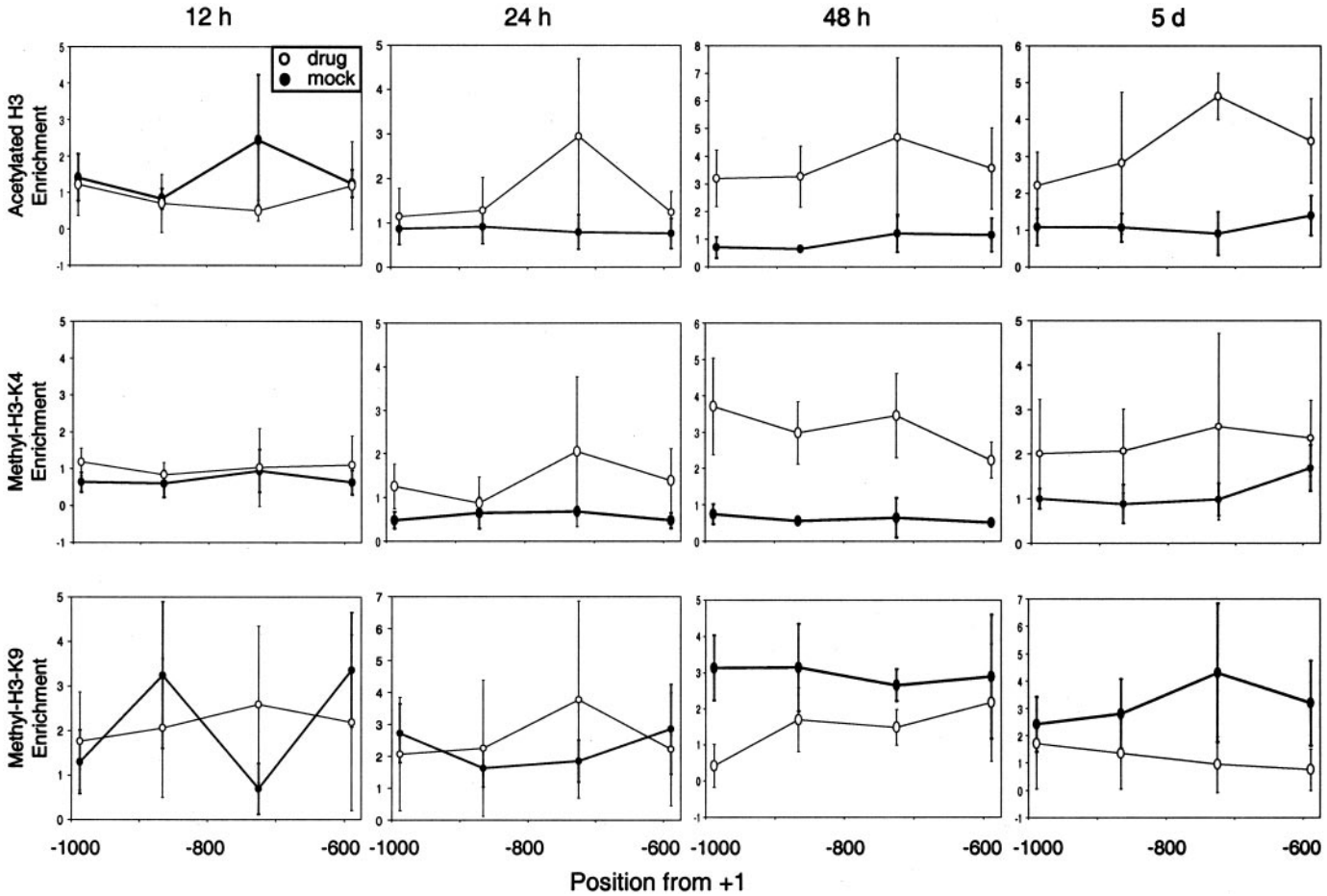

Fig. 4. Treatment with 5-Aza-dC reverses all components of the histone code examined at a hypermethylated *hMLH1* promoter by 48 h. The data represent two independent time course experiments in which RKO cells were treated with 1 μM 5-Aza-dC (or mock-treated) and harvested at each time point shown for ChIP analysis. A total of four to seven PCR analyses were performed on the immunoprecipitated DNA from each time point. Each point on the graphs represents the average value of enrichment, and each *error bar* indicates the SD from the mean. ○ represents data from RKO cells treated with 5-Aza-dC. ● represents data from mock-treated RKO cells. Data from a 5-day time point served as positive controls to ensure that drug treatment was effective. The *broken horizontal bars* under the *hMLH1* promoter schematic in Fig. 1*A* indicate the location of the primer sets used in this ChIP and PCR analysis.

Neurospora (10) and *Arabidopsis* (11) suggest the opposite and point to a role for methyl-H3-K9 in targeting and maintaining DNA methylation. Our data stress the importance of identifying the enzymes responsible for modifying the histones in the setting of mammalian gene promoters and developing histone methyltransferase inhibitors to formally test relationships between histone modifications and DNA methylation in mammalian cells.

A second and more indirect mechanism may better fit the changes we have observed and relate to an important new view of relationships between histone code parameters and gene transcription (19–21). In this scenario, DNA demethylation leads to gene reactivation, which in turn, leads to reversal of key elements of the histone code. This possibility is supported by our temporal data and by recent exciting findings in *Arabidopsis* (21) and *Drosophila* (20) by others. Johnson *et al.* (21) report that loss of DNA methylation itself does not lead to a decrease in methyl-H3-K9; rather, only at loci where reactivation of transcription occurs because of loss of DNA methylation does methyl-H3-K9 decrease. They postulate that methyl-H3-K9 may be replaced by replication-independent deposition of new nucleosomes containing variant histone H3.3 once transcription occurs (21), a concept suggested by studies from Ahmad and Henikoff (20) in *Drosophila*. In light of these findings, our data could be interpreted as showing that 5-Aza-dC leads to demethylation of the DNA, which causes reactivation of *hMLH1* gene transcription and, possibly, subsequent deposition of H3.3. The newly deposited variant histones would lack methyl-H3-K9 and could undergo posttranslational modification, including methylation at K4 or acetylation, resulting in a heritable histone code that supports active transcription at the *hMLH1* promoter. This type of mechanism could also help to explain our previous findings that TSA alone cannot reactivate hypermethylated genes in cancer but can synergize with low doses of 5-Aza-dC to reactivate such genes (12, 13). In this model, TSA may be working by facilitating the acetylation of the newly deposited histones, thus helping to augment newly initiated transcription.

Although additional studies must continue to verify the above proposed sequence of events, our new findings are important to multiple aspects of abnormal, epigenetically mediated gene silencing in cancer. Pooling all of the available data, including ours and those from studies in *Neurospora* (10) and *Arabidopsis* (11, 21), the following sequence of events is a plausible model for DNA methylation-mediated silencing of tumor suppressor genes in cancer. Our extensive histone code map along the *hMLH1* promoter in SW480 cells suggests that enrichment of acetylated H3 and methyl-H3-K4 within and upstream of promoter CpG islands could protect the islands at normally expressed mammalian genes from DNA hypermethylation, similar to the postulated methyl-H3-K4- and acetylation-mediated protection from transcriptional repression that has been suggested to occur in chickens (4) and yeast (5). Such protection may be lost in some

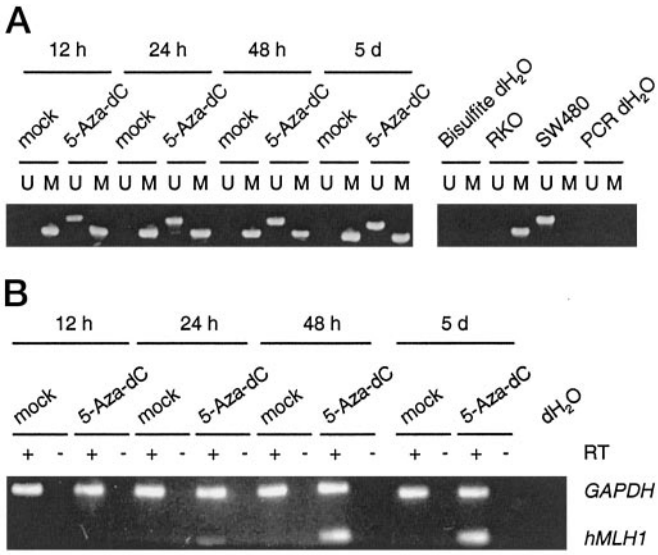

Fig. 5. Treatment with 5-Aza-dC initiates demethylation by 12 h and transcription by 24 h at a hypermethylated *hMLH1* promoter. RKO cells were treated with 1 μM 5-Aza-dC and harvested at the indicated time points. *A*, MSP analysis of *hMLH1*. A *doubled line* above the *hMLH1* promoter schematic in Fig. 1*A* indicates the region examined by MSP. Methylation was detected by the presence of a PCR product amplified by methylation-specific primers in the M lanes. Demethylation was detected by PCR products amplified by unmethylated-specific primers in the U lanes. Bisulfite dH_2O denotes bisulfite-treated dH_2O, which served as a negative control for the treatment. RKO and SW480 served as positive controls for the methylated and unmethylated PCR reactions, respectively. *B*, reverse transcriptase-PCR analysis of *hMLH1* expression. *GAPDH* expression served as a loading control. Five-day mock- and 5-day 5-Aza-dC-treated RKO cells served as negative and positive controls, respectively, for *hMLH1* expression.

Table 1 *Summary of time course data*

Changes observed	0 h	12 h	24 h	48 h	5 d
DNA demethylation	No	Yes	Yes	Yes	Yes
Gene reexpression	No	No	Yes	Yes	Yes
Acetylated H3	↓[a]	↓	↓	↑	↑
Methyl-H3-K4	↓	↓	↓	↑	↑
Methyl-H3-K9	↑	↑	↑	↓	↓

[a] ↓, depletion; ↑, enrichment.

cancers at selected sites because these key components of the histone code break down, allowing histone deacetylation to occur, methyl-H3-K9 to spread into the promoter, and aberrant DNA hypermethylation of the CpG island and silencing to result. Our data suggest that DNA hypermethylation firmly maintains this new heritable silenced state by repressing transcription and, directly or indirectly, sustaining these key elements of a repressive histone code. Importantly, 5-Aza-dC is able to disrupt this established heritable state of the histones. These findings stress the usefulness of this drug for dissecting the basic relationships between DNA methylation and histone modifications for their contribution to gene expression patterns in normal and disease states, as well as the possibilities for reversing DNA hypermethylation and repressive components of the histone code for prevention and treatment of cancer.

Acknowledgments

We thank Drs. Kurtis E. Bachman and Kam-Wing Jair for helpful suggestions during the course of these studies. We also thank Dr. Elizabeth E. Cameron for immunofluorescence data mentioned in the text.

References

1. Baylin, S. B., and Herman, J. G. DNA hypermethylation in tumorigenesis: epigenetics joins genetics. Trends Genet., *16:* 168–174, 2000.
2. Jones, P. A., and Laird, P. W. Cancer epigenetics comes of age. Nat. Genet., *21:* 163–167, 1999.
3. Jenuwein, T., and Allis, C. D. Translating the histone code. Science (Wash. DC), *293:* 1074–1080, 2001.
4. Litt, M. D., Simpson, M., Gaszner, M., Allis, C. D., and Felsenfeld, G. Correlation between histone lysine methylation and developmental changes at the chicken β-globin locus. Science (Wash. DC), *293:* 2453–2455, 2001.
5. Noma, K., Allis, C. D., and Grewal, S. I. Transitions in distinct histone H3 methylation patterns at the heterochromatin domain boundaries. Science (Wash. DC), *293:* 1150–1155, 2001.
6. Peters, A. H., Mermoud, J. E., O'Carroll, D., Pagani, M., Schweizer, D., Brockdorff, N., and Jenuwein, T. Histone H3 lysine 9 methylation is an epigenetic imprint of facultative heterochromatin. Nat. Genet., *30:* 77–80, 2002.
7. Heard, E., Rougeulle, C., Arnaud, D., Avner, P., Allis, C. D., and Spector, D. L. Methylation of histone H3 at Lys-9 is an early mark on the X chromosome during X inactivation. Cell, *107:* 727–738, 2001.
8. Boggs, B. A., Cheung, P., Heard, E., Spector, D. L., Chinault, A. C., and Allis, C. D. Differentially methylated forms of histone H3 show unique association patterns with inactive human X chromosomes. Nat. Genet., *30:* 73–76, 2002.
9. Xin, Z., Allis, C. D., and Wagstaff, J. Parent-specific complementary patterns of histone H3 lysine 9 and H3 lysine 4 methylation at the Prader-Willi syndrome imprinting center. Am. J. Hum. Genet., *69:* 1389–1394, 2001.
10. Tamaru, H., and Selker, E. U. A histone H3 methyltransferase controls DNA methylation in *Neurospora crassa*. Nature (Lond.), *414:* 277–283, 2001.
11. Jackson, J. P., Lindroth, A. M., Cao, X., and Jacobsen, S. E. Control of CpNpG DNA methylation by the Kryptonite histone H3 methyltransferase. Nature (Lond.), *416:* 556–560, 2002.
12. Cameron, E. E., Bachman, K. E., Myohanen, S., Herman, J. G., and Baylin, S. B. Synergy of demethylation and histone deacetylase inhibition in the re-expression of genes silenced in cancer. Nat. Genet., *21:* 103–107, 1999.
13. Suzuki, H., Gabrielson, E., Chen, W., Anbazhagan, R., van Engeland, M., Weijenberg, M. P., Herman, J. G., and Baylin, S. B. A genomic screen for genes up-regulated by demethylation and histone deacetylase inhibition in human colorectal cancer. Nat. Genet., *31:* 141–149, 2002.
14. Herman, J. G., Umar, A., Polyak, K., Graff, J. R., Ahuja, N., Issa, J. P., Markowitz, S., Willson, J. K., Hamilton, S. R., Kinzler, K. W., Kane, M. F., Kolodner, R. D., Vogelstein, B., Kunkel, T. A., and Baylin, S. B. Incidence and functional consequences of hMLH1 promoter hypermethylation in colorectal carcinoma. Proc. Natl. Acad. Sci. USA, *95:* 6870–6875, 1998.
15. Herman, J. G., Graff, J. R., Myohanen, S., Nelkin, B. D., and Baylin, S. B. Methylation-specific PCR: a novel PCR assay for methylation status of CpG islands. Proc. Natl. Acad. Sci. USA, *93:* 9821–9826, 1996.
16. Magdinier, F., and Wolffe, A. P. Selective association of the methyl-CpG binding protein MBD2 with the silent p14/p16 locus in human neoplasia. Proc. Natl. Acad. Sci. USA, *98:* 4990–4995, 2001.
17. Nguyen, C. T., Gonzales, F. A., and Jones, P. A. Altered chromatin structure associated with methylation-induced gene silencing in cancer cells: correlation of accessibility, methylation, MeCP2 binding and acetylation. Nucleic Acids Res., *29:* 4598–4606, 2001.
18. Jones, P. A., and Baylin, S. B. The fundamental role of epigenetic events in cancer. Nat. Rev. Genet., *3:* 415–428, 2002.
19. Goll, M. G., and Bestor, T. H. Histone modification and replacement in chromatin activation. Genes Dev., *16:* 1739–1742, 2002.
20. Ahmad, K., and Henikoff, S. The histone variant H3.3 marks active chromatin by replication-independent nucleosome assembly. Mol. Cell, *9:* 1191–1200, 2002.
21. Johnson, L., Cao, X., and Jacobsen, S. Interplay between two epigenetic marks: DNA methylation and histone H3 lysine 9 methylation. Curr. Biol., *12:* 1360–1367, 2002.

Dependence of Histone Modifications and Gene Expression on DNA Hypermethylation in Cancer

Jill A. Fahrner, Sayaka Eguchi, James G. Herman, et al.

Cancer Res 2002;62:7213-7218.